Catalytic Properties of Iron Oxides. II.[1] Isotopic Exchange of Oxygen, Oxidation of Carbon Monoxide, and Reduction-Oxidation Mechanism

Kanji SAKATA, Fumio UEDA, Makoto MISONO,* and Yukio YONEDA

Department of Synthetic Chemistry, Faculty of Engineering, The University of Tokyo, Hongo, Bunkyo-ku, Tokyo 113

(Received May 4, 1979)

The reactivity and mobility of the lattice oxygen of iron oxide, in particular γ-Fe_2O_3, has been investigated by ^{18}O-exchange with CO_2 and CO oxidation by $^{18}O_2$. The low mobility of the lattice oxygen is in agreement with the reduction-oxidation mechanism of γ-Fe_2O_3 bulk, which proceeds by Fe ion migration without diffusion of the lattice oxygen. The rapid diffusion of the Fe ion makes the redox cycles of γ-Fe_2O_3 easy and explains, together with the cation deficient structure, the high reactivity and selectivity of lattice oxygen. Thus, γ-Fe_2O_3 may be regarded as a new prototype of selective catalyst for allylic oxidation.

Iron oxide catalyst is widely used either as a single metal oxide or as a mixed oxide in industrial processes such as dehydrogenation (*e.g.* ethylbenzene to styrene and methanol to formaldehyde), the water gas shift reaction, and the reduction of nitrogen monoxide.[2] Among the oxides of the first transition metals, iron oxide exhibits intermediate activity in the complete oxidation of methane, carbon monoxide, and isotopic equilibration of oxygen,[3] but is not a good catalyst in the partial oxidation of hydrocarbons.[4,5]

It has been demonstrated that iron oxide becomes very active and selective in the oxidative dehydrogenation of butenes, when the structure of iron oxide is transformed from the α-form (hematite; a corundum structure) to the γ-form (maghemite; an inverse spinel).[6] This high activity and selectivity of γ-Fe_2O_3 was confirmed in catalytic reactions in both pulse and flow reactors at 250—300 °C.[6c] This temperature range is considerably lower than that employed for Bi_2O_3–MoO_3 catalysts.[7]

The importance of structural factors and the oxidation state of iron oxide catalysts may be inferred from the following. In the dehydrogenation of ethylbenzene, the addition of alkali metal to or the pre-reduction of iron oxide increases the selectivity significantly. It has been suggested that this effect is not only electronic but also structural.[8] In this reaction, the oxidation state of iron oxide has been reported to be important.[9] Changes in structure under the reaction conditions of oxidative dehydrogenation of butenes was observed by Sazonova *et al.*,[10] who attributed this change to the reduction of α-Fe_2O_3 to Fe_3O_4. This change is probably however a transformation to γ-Fe_2O_3 based on our results. In ferrite catalysts, distribution of metal ions into tetrahedral (Td) sites and octahedral (Oh) sites appears to be connected to the catalytic activity for the dehydrogenation of butenes.[11]

In a previous report the catalytic activity of iron oxide in the oxidation of butene was investigated as a function of the structure and oxidation state, the results of which are summarized as follows:

(i) The activity for butadiene formation varies markedly with the bulk structure and the oxidation state, *i.e.* γ-$Fe_2O_3 > \alpha$-$Fe_2O_3 \gg Fe_3O_4$.[6]

(ii) Lattice oxygen is the reactive oxygen species and the redox mechanism which comprises reduction-oxidation cycles of iron oxide is operative.[6]

(iii) The allylic species is probably the reaction intermediate in view of the substituent effect of the reactant.[6b]

The last two facts apparently coincide with those reported for Bi_2O_3–MoO_3.** In Bi_2O_3–MoO_3, oxygen tracer studies coupled with kinetic studies have revealed that oxidation proceeds by redox cycles of catalyst and the lattice oxygen is directly involved in the reaction.[7,12] The importance of the high mobility of oxygen in the bulk oxide has been pointed out in this oxide and also for other related mixed oxides.[13] These mixed oxides form one group of oxidation catalysts, in which Bi_2O_3–MoO_3 may be considered a prototype.

The aim of the present study has been to investigate the reactivity and mobility of the lattice oxygen of iron oxide, particularly in γ-Fe_2O_3, and to elucidate the redox process which is pertinent to the catalytic oxidation. Stress has been placed on the similarity and contrasts of iron oxide to Bi_2O_3–MoO_3, to provide a new prototype of oxidation catalyst, comprising a single metal oxide.

Experimental

Apparatus. A conventional pulse reactor and a closed circulation reactor were used for the reactions. The pulse technique used was the same as described elsewhere.[6] Oxygen impurities in the He carrier gas were removed by a molecular-sieve trap kept at the temperature of liquid-nitrogen. The closed circulation system, equipped with a mercury manometer, a magnetic circulation pump, and a gas-sampling valve for the measurement of mass spectra, had a volume of *ca.* 200 cm^3 and was readily evacuated to 10^{-3} Pa by a rotary pump and an oil diffusion pump.

Catalysts and Reagents. α-Fe_2O_3 (BET surface area: 10 $m^2\,g^{-1}$) was prepared from $Fe(NO_3)_3$ (Kishida Chemical Co.) as described previously.[6] γ-Fe_2O_3 was prepared from α-Fe_2O_3 by two methods. In the pulse reactor, α-Fe_2O_3 was reduced

** Both iron oxide and Bi_2O_3–MoO_3 are selective catalysts for butene oxidation, but the former is not a selective catalyst for the oxidation of propene to acrolein. This difference may be attributed to the low activity of iron oxide in the reaction step of oxygen addition to the allylic intermediate. Both oxides are however very similar for the allyl formation (abstraction of an allyl hydrogen by oxygen on metal oxides). This step is often considered the key reaction of allylic oxidation.

by CO pulses to Fe_3O_4 and then re-oxidized by O_2 or N_2O pulses to γ-Fe_2O_3 at 200—300 °C. The structures of α- and γ-Fe_2O_3 prepared by this procedure were confirmed by X-ray powder diffraction patterns and Mössbauer spectra. γ-Fe_2O_3 was also prepared in the closed circulation system by reducing α-Fe_2O_3 to Fe_3O_4 with pure CO or mixtures of CO and CO_2, followed by re-oxidation with O_2. As described in the following section the reduction of iron oxide by CO in a closed system appeared to partially form Fe metal and Fe carbide.

O_2 enriched in ^{18}O(^{18}O: 20 or 70 atom %) was purchased from Japan Radioisotope Association. $C^{18}O_2$(^{18}O: 10 or 35 atom %) was prepared by oxidizing CO with ^{18}O-enriched O_2 over iron oxide at 300 °C and used without further treatment.

Procedures. Both ^{18}O-exchange between CO_2(or O_2) and iron oxide and CO oxidation over iron oxide using $^{18}O_2$ were conducted in the closed circulation reactor. Prior to reaction, the iron oxide samples (300 or 600 mg) were evacuated in the closed system for 1 h at 300 °C, treated with pure O_2 (13 kPa) at 300 °C (with circulation and a liquid nitrogen trap), and finally evacuated for 1 h at the reaction temperature. ^{18}O distributions in CO, O_2, and CO_2 in the gas phase was analyzed by a mass spectrometer (Hitachi Co, Ltd.) after intermittent sampling. After the run, the catalyst was subjected to X-ray powder diffraction analysis by a Geigerflex ECP-TG (Rigaku Denki Co.) with Cu $K\alpha$ irradiation. Analysis showed that the structure of the catalyst did not change before and after the run.

Results

Oxygen-18 Exchange between CO_2 or O_2 and Iron Oxide. The reactivity of the lattice oxygen of the iron oxide was investigated by ^{18}O-exchange between ^{18}O-labeled CO_2 (10 Torr) and iron oxide (600 mg). Figure 1 illustrates the changes of ^{18}O content (atomic fraction) in CO_2 with reaction time, where the ^{18}O contents relative to the initial ^{18}O content are given. The reaction temperature was raised in steps from 150 °C to 300 °C as indicated in the figure. The times required to raise the temperature from 150 to 220 °C and from 220 to 300 °C were 10—15 min each.

From Fig. 1 it may be seen that the ^{18}O content became constant within 5 min after the introduction of CO_2 over both α- and γ-Fe_2O_3 at 150 °C. In all runs,

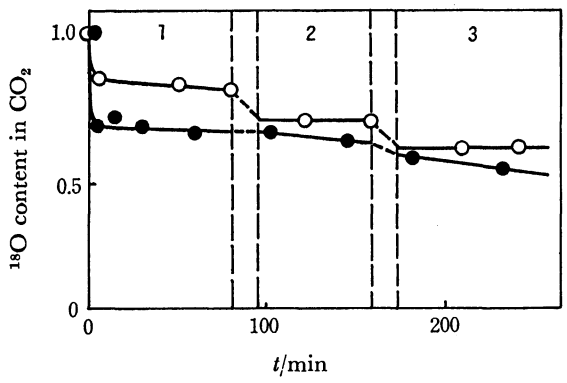

Fig. 1. Isotopic exchange of oxygen between $C^{18}O_2$ and Fe_2O_3.
React. temp (°C), 1: 150, 2: 220, 3: 300.
○: γ-Fe_2O_3, ●: α-Fe_2O_3, Fe_2O_3: 0.6 g, P_{CO_2}: 1 cmHg. ^{18}O content is relative to the initial content.

the ^{18}O distributions in CO_2 in the gas phase were always in equilibrium, *i.e.* $[C^{16}O^{18}O]^2/\{[C^{18}O_2]\times[C^{16}O_2]\}=4$. In the case of α-Fe_2O_3, a small decrease of the ^{18}O content in CO_2 with reaction time was observed at 220 and 300 °C (Fig. 1), but this decrease was very small and negligible compared with the total change of the ^{18}O content in CO_2.

The indication is that oxygens of the iron oxides exchange rapidly with CO_2, but the degree of exchange is very small: 1.4 cm^3 NTP g^{-1} (0.5) for α-Fe_2O_3 and 0.9 cm^3 NTP g^{-1} (0.3) for γ-Fe_2O_3 at 150 °C. At 300 °C, the values are 3.5 (1.3) and 2.7 cm^3 NTP g^{-1} (1.0) for α- and γ-Fe_2O_3, respectively. The numbers in parentheses are the amounts of exchangeable oxygen in terms of surface layers, calculated by assuming the number of oxygen in one layer to be 1.5×10^{19} atom m^{-2} (see Discussion). Consequently, the amounts of exchangeable oxygen are comparable to or smaller than one surface layer.

Oxygen exchange between $^{18}O_2$ and iron oxide was very slow, *e.g.* 0.6 cm^3 NTP g^{-1} (0.2 surface layer) exchanged after 4 h at 300 °C and the isotope distributions in O_2 remained far from equilibrium, indicating that isotopic equilibration of O_2 was also very slow. Therefore, the activation of molecular oxygen on iron oxides in the fully oxidized state is a slow process.

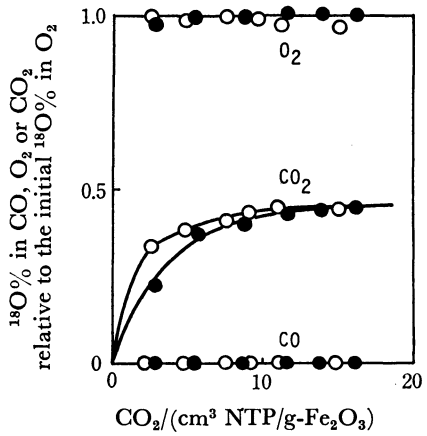

Fig. 2. ^{18}O contents in CO, O_2 and CO_2 during CO oxidation by $^{18}O_2$ over α- and γ-Fe_2O_3 at 150 °C.
○: γ-Fe_2O_3, ●: α-Fe_2O_3.

CO Oxidation by $^{18}O_2$. CO oxidation by $^{18}O_2$ was conducted at 150 °C, to determine the amount of oxygen atoms in iron oxide participating in catalytic oxidation. The ^{18}O contents in CO, O_2, and CO_2 are plotted in Fig. 2 as a function of the amount of CO_2 produced, where the ^{18}O contents are all normalized to the initial ^{18}O content in O_2. Over both α- and γ-Fe_2O_3, the ^{18}O content in CO_2 produced at the initial stage was low and then gradually increased with reaction time as shown in Fig. 2. The ^{18}O distributions in CO_2 were always in equilibrium during the reaction. In contrast to CO_2, ^{18}O-exchange between CO or O_2 and iron oxide did not occur at all, as seen from the constant ^{18}O contents in O_2 and CO during the reaction. Isotopic equilibration in O_2 was also absent.

From these data, it is possible to calculate the amount

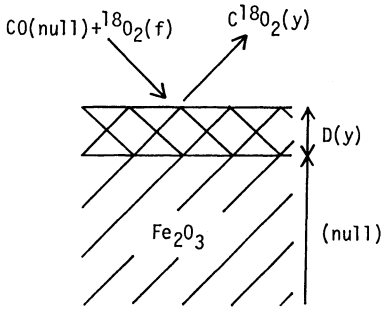

Fig. 3. Model for calculation of the amount of lattice oxygen participating in CO oxidation by $^{18}O_2$.
( ): ^{18}O content (%)
D: the amount of lattice oxygen participating in CO oxidation (see text).
f and y are ^{18}O% in O_2 and CO_2, respectively.

of oxygen atoms in iron oxide, which participate in the CO oxidation. Since the ^{18}O-exchange between CO_2 and iron oxide was very rapid as shown in Fig. 1, the amount of oxygen atoms calculated here includes those which participated only in the ^{18}O-exchange between CO_2 and iron oxide, in addition to the lattice (or surface) oxygen atoms which were incorporated into CO_2 directly by the oxidation reaction. In other words, only the upper limit of the lattice (or surface) oxygen atoms which have participated directly in CO oxidation can be determined. The calculation was conducted in the following manner. Since the oxygen exchange between the surface and CO_2 is rapid, it is reasonable to place the ^{18}O content in the catalyst surface equal to the ^{18}O content in CO_2 at each reaction time. The model for CO oxidation by $^{18}O_2$ over iron oxide is shown in Fig. 3. It was assumed that the surface layer of the catalyst which participates equally in the reaction has a uniform ^{18}O concentration to a depth of D (expressed in cm^3 NTP g^{-1}) and that the lattice oxygen in the bulk deeper than this layer (depth$>D$) does not participate in the reaction (^{18}O: 0%). The method reported by Miura *et al.*[14] was subsequently applied for the calculation, where the contribution from ^{18}O-exchange between CO_2 and catalyst surface was additionally taken into account. In Fig. 3, p, y, and f represent the amount (cm^3 NTP g^{-1}) of CO_2 produced, the ^{18}O content (%) in CO_2 at reaction time t (min), and the ^{18}O content (%) in O_2, respectively. The mass balance of the ^{18}O in the catalyst surface layer D at reaction time t is represented by Eq. 1.

$$D\mathrm{d}y = f\mathrm{d}p - 2\mathrm{d}(py) \quad (1)$$

$$p = D \cdot y/(f-2y) \quad (2)$$

Integration of Eq. 1 at the initial conditions of $p=0$ and $y=0$ gives Eq. 2. Equation 2 shows that a plot of p against $y/(f-2y)$ gives a slope ($=D$) which represents the amount of oxygen in the catalyst participating in CO oxidation (oxygen atom, cm^3 NTP g^{-1}). The results in Fig. 2 are plotted in Fig. 4, according to Eq. 2. From the slopes of the linear plots in this figure, the amounts of oxygen at 150 °C have been calculated as 3.3 (1.2) and 2.0 cm^3 NTP g^{-1} (0.7 surface layers) for α- and γ-Fe_2O_3, respectively (numbers in parentheses are in terms of surface layers). These values are comparable with the amount of exchangeable oxygen with

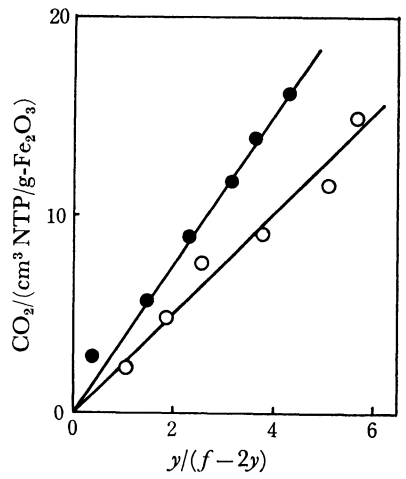

Fig. 4. Plots of CO_2 produced *vs.* $y/(f-2y)$ (Eq. 2) for the calculation of the amount (D) of lattice oxygen participating in CO oxidation by $^{18}O_2$.
○: γ-Fe_2O_3, ●: α-Fe_2O_3
Slope of linear plot gives D.
f and y are the same as in Fig. 3.

CO_2 and demonstrate that the amount of oxygen participating directly in the reaction is at most one or two surface layers even during the CO oxidation.

Reduction-Oxidation (Redox) Mechanism of γ-Fe_2O_3. The reduction and re-oxidation of the bulk of iron oxide was very rapid, and this rapid redox process appeared connected with the high activity and selectivity observed for oxidative dehydrogenation.[6] The results indicate however that the lattice oxygen has low mobility in the bulk. Therefore, an attempt was made to determine which ion (O^{2-} or Fe^{3+}) diffused during the redox process. The method is schematically drawn in Scheme 1. γ-$Fe_2{}^{18}O_3$ prepared by the re-oxidation of Fe_3O_4 by

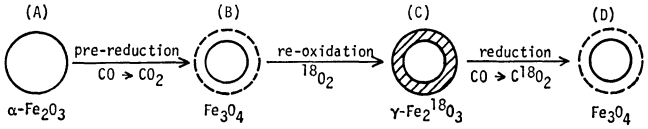

Scheme 1. Changes of one sample particle are schematically drawn. Shaded area is the layer formed by re-oxidation, which is eliminated by subsequent reduction.

$^{18}O_2$ (Scheme 1, A→B→C) was gradually reduced by CO (Scheme 1, C→D), in which the ^{18}O contents of CO_2 produced were measured as a function of the degree of reduction, x in γ-Fe_2O_{3-x}. The degree of reduction, x, has been evaluated from the amount of CO_2 produced (x of Fe_3O_4=0.33). The ^{18}O recovery is defined as

$$^{18}\mathrm{O\ recovery} = 2 \times [^{18}\mathrm{O}\% \text{ in } CO_2 \text{ produced during the reduction by CO}]/[^{18}\mathrm{O}\% \text{ in } O_2 \text{ used for the re-oxidation}] \quad (3)$$

The ^{18}O recovery is expected to be as follows, depending on the rate of oxygen diffusion. (1) If lattice oxygen does not migrate during the $^{18}O_2$ re-oxidation and the subsequent CO reduction, ^{18}O should be uniformly contained only in the surface layer formed by the re-oxidation, the ^{18}O content in this layer being identical

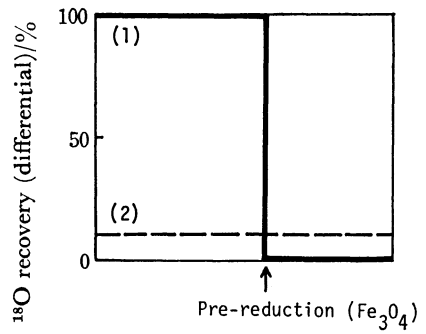

Fig. 5. ^{18}O recovery (differential) expected for the process C→D in Scheme 1 for two extreme cases.
(1) No oxygen diffusion,
(2) rapid oxygen diffusion.

to that in $^{18}O_2$ used for the re-oxidation. Therefore, the differential ^{18}O recovery, which is defined as the ^{18}O recovery for a small increment of CO_2 formation, should be 100% until the γ-$Fe_2{}^{18}O_3$ is reduced to the state of the pre-reduction (Scheme 1, B), and nil (zero) on further reduction (Fig. 5, full line). (2) If lattice oxygen diffuses very rapidly (complete mixing of lattice oxygens), the differential ^{18}O recovery is constant and equal to the amount determined by the reaction stoichiometry: 11% for γ-Fe_2O_3 in the present experiment (Fig. 5, broken line). Thus the ^{18}O recovery reflects the change in the ^{18}O concentration from the surface to the center and, therefore, the rate of diffusion of the oxide ion (Fig. 6).

In Exp. 1, both the CO reduction and $^{18}O_2$ re-oxidation were performed in a closed circulation system at 250 °C. The ^{18}O recovery was 66% after corrections for the ^{18}O-exchange between iron oxide and CO_2. The migration of lattice oxygen was slow but not negligible. This rather low recovery of ^{18}O may be attributed to a diffusion of lattice oxygen accelerated by the increase of temperature caused by the exothermic re-oxidation step. Therefore, the reaction temperature of the re-oxidation step was lowered from 250 °C to 150 °C in Exp. 2, but there was only a small increase in ^{18}O recovery (65—71%). Another possible explanation for the low ^{18}O recovery is the formation of iron metal or iron carbide in the reduction step ($CO+Fe_2O_3 \rightarrow CO_2+Fe$, FeC_n). In Exp. 3, reduction was carried out with a mixture of CO and CO_2. The ^{18}O recovery increased slightly (72—73%) but the formation of iron metal and iron carbide was still indicated since the reduction-oxidation was not completely stoichiometric and a small amount of CO_2 was formed on re-oxidation. Finally, CO reduction (both pre-reduction and final reduction) was performed with the pulse method and re-oxidation by $^{18}O_2$ with the closed circulation system (Exp. 4), by transferring the sample between the two systems without exposing it to air. In this method, the reduction and subsequent re-oxidation of α-$Fe_2O_3 \rightarrow Fe_3O_4 \rightarrow \gamma$-$Fe_2O_3$ was confirmed at each step stoichiometrically and by X-ray diffraction analysis and Mössbauer spectroscopy. Further, there was no change in surface area.

As shown in Fig. 6, by using γ-$Fe_2{}^{18}O_3$ thus prepared the ^{18}O recovery increased to 91% at the reduction stage of $x=0.25$ and was 83% at $x=0.33$ (reduction to Fe_3O_4). Therefore, it may be assumed that little diffusion of lattice oxygen took place during the redox cycle.

Exp.	Redox conditions: Re-oxid.	Red.	Total recovery of ^{18}O (%)
	$^{18}O_2$	CO	
1	250°C	250°C	62 - 66
	C	C	
	$^{18}O_2$	CO	
2	150°C	230°C	65 - 71
	C	C	
	$^{18}O_2$/He	CO+CO_2	
3	200°C	270°C	72 - 73
	C	C	
	$^{18}O_2$	CO/He	
4	200°C	300°C	82 - 83
	C	P	

C: circulation system
P: pulse reactor

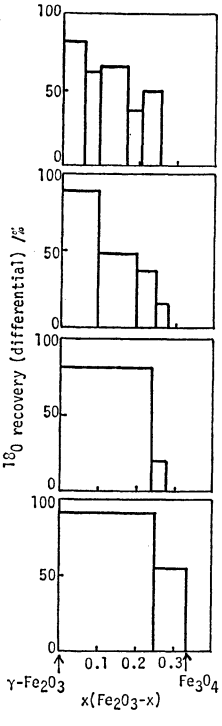

Fig. 6. ^{18}O recovery into CO_2 for the process, γ-$Fe_2{}^{18}O_2 + CO \rightarrow Fe_3O_4 + C{}^{18}O_2$.

Discussion

Mobility of Lattice Oxygen in Iron Oxide. As shown by the isotopic exchange of oxygen with CO_2 (Fig. 1) and the CO oxidation by $^{18}O_2$ (Figs. 2—4), the amount of lattice (surface) oxygen of iron oxide, which participates in these reactions was 0.9—3.5 cm^3 NTP/g-Fe_2O_3. This amount is equivalent to 0.4—1.4% of the total lattice oxygen and is very small compared with Bi_2O_3–MoO_3, for which the amount of oxygen participating in CO oxidation was about 20% of total lattice oxygen.[14] A remarkable contrast exists, therefore, between iron oxide and Bi_2O_3–MoO_3, although both catalysts are very similar.

Although iron oxide is not very active for the activation of the O_2 molecule below 300 °C, as seen from the very small rate observed in the ^{18}O-exchange with O_2, the ^{18}O-exchange between surface oxygen and CO_2 was rapid and equilibrium was reached almost instantaneously. The agreement of the amounts of exchangeable oxygen calculated for CO_2 exchange (Fig. 1) and CO oxidation (Fig. 4) may be due to the fact that both were determined by the same reaction, that is, the ^{18}O-exchange between CO_2 and iron oxide surface. This reaction is generally considered to proceed *via* a surface carbonate complex.[15] Over iron oxide the formation of surface carbonate from CO_2 has actually been detected

by infrared spectrometry.[16]

The amount of exchangeable oxygen of iron oxide calculated from the ^{18}O concentration of CO_2 after a long period of the reaction was 3.5 and 2.7 cm^3 NTP/g-Fe_2O_3 at 300 °C for α- and γ-Fe_2O_3, respectively. These values may be represented in terms of the number of surface layers and compared with those reported in the literature. Assuming the surface of iron oxide is composed of the maximum packing of oxide ion, the surface density is thus 1.5×10^{19} atom m^{-2} for the (111) surface (radius of O^{2-}; 1.40 Å). The actual surface density of oxide ion may be lower than this value, since the metal oxide surface is not fully covered with oxide ion. In general, the surface atom density is given as $1—2\times10^{19}$ atom m^{-2}.[17] Assuming the value of 1.5×10^{19} atom m^{-2}, the exchangeable oxygen at 300 °C obtained in the present work corresponds to 1.3 and 1.0 surface layers for α- and γ-Fe_2O_3, respectively. Based on the work of Nováková using Winter's data,[18] the amount of oxygen exchangeable with O_2 is 1.5—4 layers for α-Fe_2O_3 at 260—400 °C, the surface oxide density being assumed 0.6×10^{19} atom m^{-2}.[15] Boreskov *et al.* reported that 1.8 surface layers were exchangeable with O_2 at 350 °C (surface oxide density; 1.28×10^{19} atom m^{-2}).[19] The present results are in reasonable agreement with those reported values and demonstrate that the diffusion of the lattice oxygen of iron oxide between the surface layer (1—2 layers) and inner bulk is a very slow process during both CO_2-oxygen isotopic exchange and CO oxidation. It is thus concluded that the mobility of the lattice oxygen is small in the bulk of iron oxide under the conditions of catalytic oxidation.

Mechanism of CO Oxidation over Iron Oxide. The oxidation state of the iron oxide catalyst may be regarded as in the fully oxidized state (Fe_2O_3) when CO oxidation is taking place, on the basis of the following. The re-oxidation process of partially reduced iron oxide by O_2 was much faster than the reduction of iron oxide by CO when measured in the circulation system. Furthermore, the rate of CO oxidation was of zero order with respect to O_2 pressure. The iron oxide catalyst under the working conditions was also found to be Fe_2O_3 (α- or γ-) in the case of the oxidative dehydrogenation of butenes in the flow reactor and the reaction was of zero order in O_2 pressure.[6c]

The reactive oxygen species on the surface of iron oxide does not desorb into the gas phase unless reaction occurs with CO to form CO_2, *i.e.* the adsorption of oxygen is irreversible and probably dissociative. In Fig. 2 neither ^{18}O-exchange between O_2, CO, and the catalyst nor the equilibration of the oxygen isotope in gaseous O_2 was observed during the CO oxidation by $^{18}O_2$. Reversible and molecularly adsorbed oxygen that might explain the facts in Fig. 2 does not seem sufficiently reactive to participate directly in the CO oxidation, even if it exists. The irreversible adsorption process of oxygen can be the oxidation of the bulk to form lattice oxygen as discussed below.

From the agreement of the reactions of butene pulses with and without O_2 it was concurred that the lattice oxygen of iron oxide is the oxygen species responsible for oxidative dehydrogenation of butenes below 300 °C.[6a] The lattice oxygen is also probably the main oxygen species involved directly in the CO oxidation. The reactivity of γ-Fe_2O_3 with CO (non-catalytic) was examined and found independent of the oxidation state from γ-Fe_2O_3 to $Fe_2O_{2.8}$. This relationship between the reactivity and the extent of reduction was very similar to that observed for the oxidative dehydrogenation of butenes. Over γ-Fe_2O_3 however the rate of oxidation of CO pulsed together with O_2 was 1.6 times greater than that without O_2, indicating that the contribution of adsorbed oxygen to the activity can not be neglected. Therefore, both the lattice oxygen and adsorbed oxygen, although these are sometimes difficult to distinguish, must be considered in the mechanism of CO oxidation. The amount of adsorbed oxygen on α-Fe_2O_3 measured by thermal desorption was approx. 2.0% of one surface layer.[20]

The CO oxidation necessitates the transfer of two electrons. In the case that lattice oxygen is the active species, a two-centered mechanism which involves two Fe^{3+} ions operates. This is a typical redox mechanism of catalytic oxidation:

$$CO + 2Fe^{3+} + O^{2-}(\text{lattice}) \longrightarrow CO_2 + 2Fe^{2+}, \quad (4)$$

$$1/2O_2 + 2Fe^{2+} \longrightarrow 2Fe^{3+} + O^{2-}(\text{lattice}). \quad (5)$$

A one-centered mechanism is for an adsorbed O^- and a Fe^{3+} ion, *i.e.* the mechanism proposed for butene dehydrogenation over ferrite catalysts:[23]

$$CO + Fe^{3+} + O^- \longrightarrow CO_2 + Fe^{2+}, \quad (6)$$

$$1/2O_2 + Fe^{2+} \longrightarrow Fe^{3+} + O^-. \quad (7)$$

In both mechanisms, CO_2 is formed by the reaction of CO and the surface oxygen species to form vacant sites which are reoccupied by the oxygen from the gas phase. The second step, (5) or (7), is always instantaneous and irreversible. The two-centered mechanism, which is probably responsible for the major part of the reaction, occurs readily, since the electron exchange in iron oxide must be very easy owing to its high electric conductivity. The ease of the electron transfer or exchange must be an important factor in some catalytic oxidations.

Reduction-Oxidation Mechanism of Bulk Iron Oxide and Catalytic Activity. In this section, the catalytic activity and the reduction-oxidation (redox) mechanism of γ-Fe_2O_3 is discussed in terms of structural characteristics, particularly the similarity of its crystal structure to Fe_3O_4. While α-Fe_2O_3 has a corundum-type structure (oxide ions form a hexagonal close-packed array with Fe^{3+} ions occupying octahedral (Oh) interstices), both γ-Fe_2O_3 and Fe_3O_4 have an inverse-spinel structure (cubic close-packed array (ccp) of oxide ion).[24] For Fe_3O_4, two-thirds of the iron cations are Fe^{3+} ions which are distributed at Td sites and Oh sites. For γ-Fe_2O_3, one-ninth of the total cation sites are vacant, probably in Oh sites.[25] The dimension of the unit cell of γ-Fe_2O_3 is 8.350 Å, which is slightly smaller than that of Fe_3O_4 (8.390 Å).

The structural characteristics suggest the following redox process between γ-Fe_2O_3 and Fe_3O_4, in which the packing structure of oxide ion remains unchanged.

The oxidation of Fe_3O_4 to γ-Fe_2O_3 proceeds by the addition of oxygen atoms on the surface to form new oxide layers which have the same packing structure as in Fe_3O_4 (ccp). This process is accompanied by the migration of iron cations from the bulk into the newly formed oxide layer to compensate for the charge, forming cation vacancies. The reduction of γ-Fe_2O_3 to Fe_3O_4 may be exactly the reverse process: removal of the oxide layer and migration of iron cations inward to fill the vacancies in the bulk. Thus, in the case of γ-Fe_2O_3, only iron cation diffuses during the reduction-oxidation of the bulk.

Experimentally this was confirmed by Exp. 4 shown in Fig. 6. The redox model of γ-Fe_2O_3, discussed above, is shown schematically in Fig. 7. The redox mechanism of γ-Fe_2O_3 bulk without the diffusion of lattice oxygen is in agreement with the results shown in Figs. 1—4, which demonstrate the very slow diffusion of lattice oxygen. Therefore, the ready interconversion between Fe^{2+} and Fe^{3+}, and the comparatively rapid diffusion of iron cations between bulk and surface layer perhaps make the redox cycles of γ-Fe_2O_3 easy. In addition to the easy redox cycles, the high energetic lattice oxygen induced by cation vacancy (low coordination number of iron)[21] may also be responsible for the high reactivity of lattice oxygen in γ-Fe_2O_3.

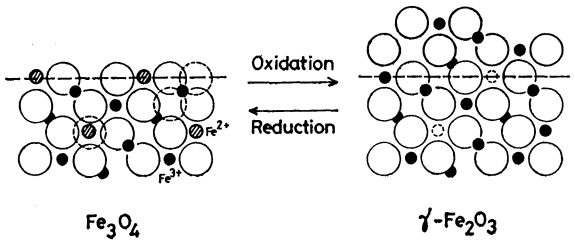

Fig. 7. Redox model of iron oxide for selective oxidation.

As discussed above, the oxidative dehydrogenation of butenes over γ-Fe_2O_3 resembles that over Bi_2O_3–MoO_3. The rapid diffusion of lattice oxygen in Bi_2O_3–MoO_3 originating from its layered structure[22] was however not observed for γ-Fe_2O_3. In the case of γ-Fe_2O_3 rapid diffusion of iron cations makes the redox cycles easy. Although the high reactivity and selectivity of both γ-Fe_2O_3 and Bi_2O_3–MoO_3 is attributed to the easy redox cycles of bulk and the high reactivity of lattice oxygen for allyl-type oxidation, their origin is quite different. Thus, γ-Fe_2O_3 may be regarded as another catalysts prototype for selective allylic oxidation.

References

1) Part I: M. Misono, Y. Nozawa, and Y. Yoneda, *Proc. 6th Int. Congr. Catal., London, 1976*, The Chemical Society (1977), p. 386.

2) M. Misono, "Kinzoku-sankabutsu To Fukugo-sankabutsu," ed by K. Tanabe, T. Seiyama, and K. Fueki, Kodansha, Tokyo (1978), p. 242.

3) G. K. Boreskov, V. V. Povovskii, and V. A. Sazonov, *Proc. 4th Int. Congr. Catal., Moskow, 1968*, Akademiai Kaido, Budapest (1971), p. 439; G. K. Boreskov, *Adv. Catal.*, **15**, 285 (1964).

4) T. Seiyama, N. Yamazoe, and M. Egashira, *Proc. 5th Int. Congr. Catal., Florida, 1972*, North-Holland Publishing Co. (1973), p. 997.

5) V. Fattore, Z. A. Fuhrman, G. Manara, and B. Notari, *J. Catal.*, **37**, 215 (1975).

6) a) M. Misono, Y. Nozawa, and Y. Yoneda, *Proc. 6th Int. Congr. Catal., London, 1976*, The Chemical Society (1977), p. 386; b) M. Misono, Y. Nozawa, and Y. Yoneda, *Shokubai*, **18**, 30 (1976); c) M. Misono, F. Ueda, K. Sakata, and Y. Yoneda, Ann. Symp. Catal. Soc. Japan, Toyama, 1977, C-17.

7) D. J. Hucknall, "Selective Oxidation of Hydrocarbons," Academic Press, London (1974).

8) E. H. Lee, *Catal. Rev.*, **8**, 285 (1974).

9) T. Hattori, Y. Murakami, M. Ii, and H. Uchida, *Kogyo Kagaku Zasshi*, **72**, 2188 (1969).

10) N. N. Sazonova, S. A. Venyaminov, and G. K. Boreskov, *Kinet. Katal.*, **14**, 1169 (1972).

11) R. J. Rennard and W. Kehl, *J. Catal.*, **21**, 282 (1971); U. S. Patent 3450787 (1969).

12) P. A. Batist, H. J. Prette, and G. C. A. Schuit, *J. Catal.*, **15**, 267 (1969); M. Egashira, H. Sumie, T. Sakamoto, and T. Seiyama, *Kogyo Kagaku Zasshi*, **73**, 860 (1970).

13) P. Pendleton and D. Taylor, *J. Chem. Soc., Faraday Trans. 1*, **72**, 1114 (1976).

14) H. Miura, Y. Morikawa, and T. Shirasaki, *Nippon Kagaku Kaishi*, **1975**, 1985.

15) J. Nováková, *Catal. Rev.*, **4**, 77 (1970).

16) V. G. Amerikov and L. A. Kasatkina, *Kinet. Katal.*, **12**, 165 (1969).

17) J. R. Anderson, "Structure of Metallic Catalysts," Academic Press Inc., London (1975), p. 296.

18) E. R. S. Winter, *J. Chem. Soc.*, **1968**, 2889.

19) G. K. Boreskov, L. A. Kasatkina, and V. G. Amerikov, *Kinet. Katal.*, **10**, 102 (1968).

20) a) T. Seiyama, "Kinzoku-sankabutsu To Sono Shokubai-sayo," Kodansha, Tokyo (1978), p. 169; b) M. Iwamoto, Y. Yoda, N. Yamazoe, and T. Seiyama, *Bull. Chem. Soc. Jpn.*, **51**, 2765 (1978).

21) Ref. 20 a), p. 41.

22) Ref. 20 a), p. 48.

23) F. E. Massoth and D. A. Scarpiello, *J. Catal.*, **21**, 294 (1971).

24) A. F. Wells, "Structural Inorganic Chemistry," 3rd ed, Clarendon Press (1967).

25) R. J. Armstrong, A. H. Morrish, and D. A. Savatzky, *Phys. Lett.*, **23**, 414 (1966). It is not confirmed which cation vacancies are distributed at Td or Oh sites. *Cf.* M. Nakahira, "Kessho Kagaku-Muki Zaishitsu Kenkyu No Shuppatsu Ten," Kodansha, Tokyo (1973), p. 185.